International Journal of Chemical, Materials and Biomolecular Sciences
ISSN: 2415-6620
Vol:7, No:10, 2013

Effect of Zr Addition on Mechanical Properties of Cr-Mo Plastic Mold Steels

Hyun-Ho Kim, Seok-Jae Lee, Oh-Yeon Lee

***Abstract*—**We investigated the effects of the additions of Zr and other alloying elements on the mechanical properties and microstructure in Cr-Mo plastic mold steels. The addition of alloying elements changed the microstructure of the normalized samples from the upper bainite to lower bainite due to the increased hardenability. The tempering temperature influenced the strength and hardness values, especially the phenomenon of 350°C embrittlement was observed. The alloy additions of Cr, Mo, and V improved the resistance to the temper embrittlement. The addition of Zr improved the tensile strength and yield strength, but the impact energy was sharply decreased. It may be caused by the formation of Zr-MnS inclusion and rectangular-shaped Zr inclusion due to the Zr addition.

***Keywords*—**Inclusions, mechanical properties, plastic mold steel, Zr addition.

I. Introduction

THE increased demand for plastic products in automotive and home appliances is due to the diversification and gentrification of product quality. Plastic mold materials used to make plastic products also require various characteristics according to the diversification of plastic products. Nowadays, Cr-Mo steels are widely used as a plastic model material. Both the alloy design and the shape control of inclusions are very important to develop a new plastic mold steel which has excellent mechanical properties after heat treatment.

The existence of MnS particles elongated during forging and hot-rolling in plastic mold steels is a cause of increasing the anisotropy of mechanical properties. The control of MnS particles with the additions of Ti, Cr, Zr, etc. has been studied to suppress the anisotropy of mechanical properties and to ensure a uniform workability [1]-[5]. Narita et al. [1] have investigated that the Zr addition controls the elongation of MnS particles by forming MnS-Zr3S4 compound in a steel containing a large amount of sulfur (0.25~0.35%S). Sawai et al. [2] have reported that the coexistence of Mn-Si oxide particles and ZrO2 particles can contribute to disperse fine MnS particles by acting as nucleation sites of MnS particles. The controlled MnS shape by the Zr addition improves the anisotropy of mechanical properties according to the distribution of MnS and Zr particles, simultaneously, the mechanical properties such as tensile strength are affected by adding Zr.

Therefore, in the present study, the effects of the additions of Zr and other alloying elements on the mechanical properties and microstructure in Cr-Mo plastic mold steels were investigated. Also the shape change of MnS particles was observed by adding Zr and other alloying elements.

Hyun-Ho Kim and Oh-Yeon Lee are with Chonbuk National University, Jeonju, Jeonbuk 561-756 Republic of Korea (e-mail: kimhh@jbnu.ac.kr, oylee@jbnu.ac.kr).

Seok-Jae Lee is with Chonbuk National University, Jeonju, Jeonbuk 561-756 Republic of Korea (corresponding author, phone: +82-63-270-2298; fax: +82-63-270-2305; e-mail: seokjaelee@jbnu.ac.kr).

II. Experimental Procedures

The chemical composition of the plastic model steels used in this study is listed in Table I. Steel ingots were prepared by a vacuum induction melting (VIM). Samples were normalized at 900°C for 90min and air-cooled. The normalized samples were heated to the temperature of A_{c3}+60°C and held for 90min, followed by oil quenching to produce a fully martensitic microstructure. Then, the samples were tempered at different tempering temperatures of 200, 400, and 600°C for 90min. The sample surface was polished and etched by 2% nital. The microstructure was observed by optical microscope (OM) and scanning electron microscope (SEM). ASTM E-8 sub-sized tensile sample was used for a room temperature tensile test. The crosshead speed was 5mm/min. The Charpy impact test according to ASTM E-23 standard was carried out at room temperature. The dimension of the V-notch Charpy sample was 10mm ×10mm ×55mm. The Rockwell hardness tester was used to measure the hardness of the samples.

TABLE I
Chemical Composition of the Steels Used in This Study (in wt.%)

Alloying element	A-1	A-2	B-1	B-2
C	0.3	0.3	0.27	0.27
Si	0.2	0.3	0.2	0.3
Mn	0.6	1.0	0.8	1.0
S	0.01	0.003	0.005	0.003
Ni	0.2	0.28	0.4	0.31
Cr	0.84	1.0	1.7	1.7
Mo	0.21	0.3	0.4	0.4
V	0.2	0.04	0.08	0.04
Zr	0.049	-	0.014	-
Fe	Bal.	Bal.	Bal.	Bal.

III. Results and Discussion

A. Microstructure and Hardness of Normalized Steels

Fig. 1 shows the optical microstructure of the normalized samples. The bainitic microstructure is commonly observed, but the volume fractions of the upper bainite (UB), lower bainite (LB), and granular bainite (GB) are varied by the different amounts of alloying elements in the samples.

The addition of Mn, which is a well-known austenite stabilizer, increases the stability of austenite and lowers the transformation temperature. The addition of Mo improves the

hardenability of steels and prevents the C diffusion by increasing the activation energy of C diffusion, resulting in the increased fraction of the MA (martensite-austenite) constituent due to the existence of C enriched austenite region [6]. Also Mo addition lowers the bainite and martensite transformation start temperatures and suppressed the formation of the UB, thus the GB and LB are easily transformed and the microstructure is refined. Similar to the Mo addition effect, Cr also improves the hardenability and suppresses the UB transformation [7]. Thus, higher volume fractions of the GB and LB can be obtained in steels containing a large amount of Cr. The addition of V accelerates the initiation of the ferrite nucleation in austenite and effectively suppresses the formation of Cr-carbonitrides at grain boundaries, which results in both the microstructure refinement and increased strength [6].

The A-1 and A-2 steels with relatively lean alloys have a higher fraction of the UB due to a higher bainite transformation temperature and a lower hardness value of HRC 30. On the other hand, The B-1 and B-2 steels which contain relatively higher amounts of alloys shows a higher fraction of the acicular LB and GB due to the retarded UB transformation and a higher hardness value of HRC 40. The dislocation density in the LB microstructure is very high and some ε and η carbides exist. The measured hardness of the normalized samples is summarized in Table II.

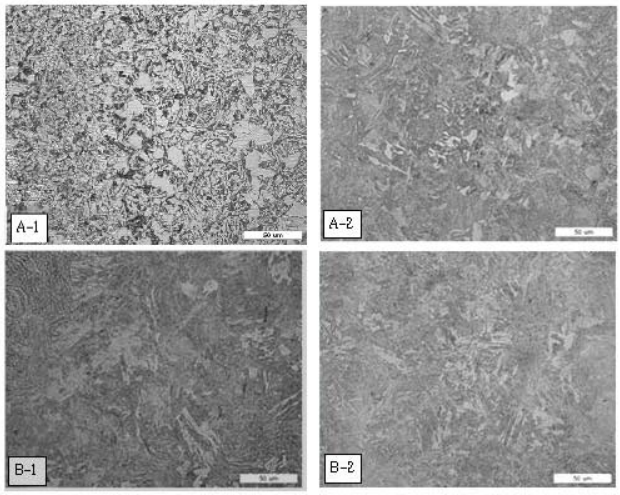

Fig. 1 Optical microstructures of the normalized steel alloys

TABLE II
AVERAGE HARDNESS VALUE (HRC) OF THE NORMALIZED STEELS

A-1	A-2	B-1	B-2
29.2	35.3	38.4	40.0

B. Mechanical Properties of Tempered Steels

Fig. 2 shows the effect of the tempering temperature on the mechanical properties of the tempered samples. The tensile strength increases as decreasing the tempering temperature, whereas the yield strength shows different tendency. The yield strength of the sample tempered at 400°C is similar or higher than the yield strength observed at 200°C, which is related to the temper embrittlement. Also the lower elongation of the sample tempered at 400°C indicates that the temperature around 400°C is included in a temper embrittlement region. It seems that the overall tensile properties are improved by the addition of Zr.

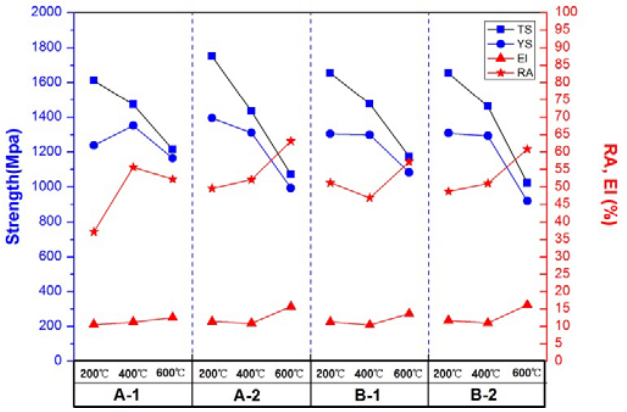

Fig. 2 Variation of the mechanical properties according to tempering temperature

Fig. 3 shows the effect of the tempering temperature on the hardness value of the tempered samples. The hardness value regardless of alloying element addition decreases as the tempering temperature increases because of the internal microstructure change. The carbon atoms enriched in octahedral sites of a body-centered tetragonal (bct) martensite are contributed to form ε-carbide precipitate during tempering at 200°C and the tetragonality of the bctmartensite is partially decreased, resulting in the decreased hardness. The average hardness value of the quenched steels is 50 HRC, but the average hardness value decreases to 46 HRC for the tempering at 200°C. And the hardness values measured in the samples tempered at 400 and 600°C are 42 and 34 HRC, respectively.

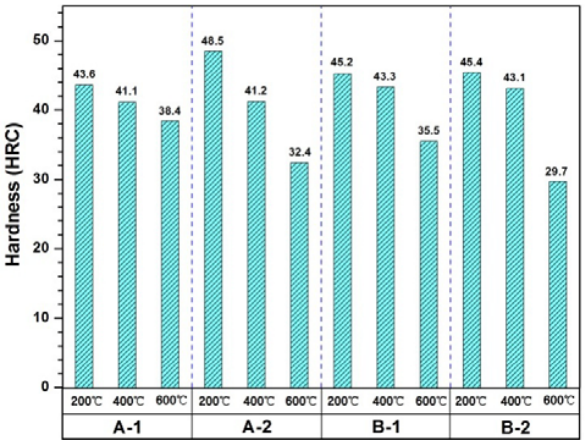

Fig. 3 Variation of the hardness with different tempering temperatures

In typical, ε-carbide is transformed to cementite and the retained austenite decomposes into ferrite and cementite as the steel is tempered from 300 to 400°C. The transformed

cementite between laths causes the temper embrittlement. The enough amount of alloying elements can maintain the tetragonality in this temperature range and prevent a sudden hardness drop. As the tempering temperature increases above 400°C, the cementite particle coarsening is accelerated and other carbides are also coarsened, which bring about the decreased hardness. It seems that the addition of Cr, Mo, and V increases the temper softening resistance and the A-1 alloy with high V content shows a good temper softening resistance.

C. Impact Toughness

The effect of the tempering temperature on the impact energy of the tempered samples is shown in Fig. 4. The impact energy of the samples tempered at 400°C indicates the lowest value. The A-1 and B-1 alloys containing Zr show lower impact energy values than the A-2 and B-2 samples regardless of the tempering temperatures. When the martensite is tempered at a temperature range of 250~400°C, the plain strain fracture toughness value is obviously decreased. This phenomenon is called 350°C embrittlement. Some factors have been investigated to cause this temper embrittlement: carbide precipitation in austenite grain boundaries [8], [9], carbide particles formed by the decomposition of retained austenite [10], [11], thermal and mechanical decomposition of retained austenite [12], grain boundary segregation of impurity elements and carbide precipitates [13]-[15]. Thomas reported that the tempering at 350°C induced the lowest impact energy in martensitic Fe-0.3C-1.0Cr-1.0Mo and Fe-0.3C-4.0Cr steels [10]. Because the cementite is precipitated from the decomposition of the film-typed austenite retained between martensite laths during tempering at 350°C. The crack is initiated in cementite particles located between martensite laths due to the stress is applied to the sample.

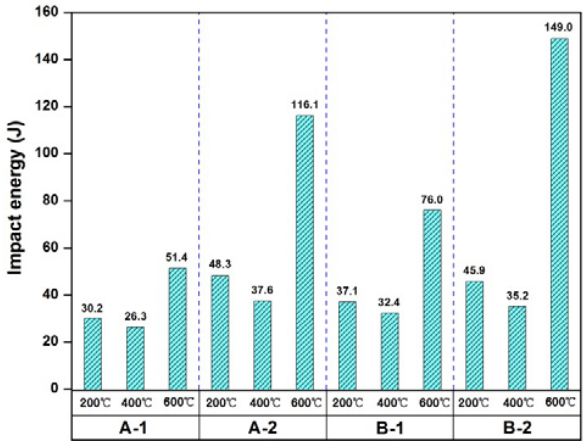

Fig. 4 Relationship between the impact energy and tempering temperature

D. Inclusion Analysis

Fig. 5 compares the inclusion shape and characteristics of the normalized samples. The elongated inclusions paralleled to the deformation direction are observed in the A-1 and A-2 steels while few inclusions are observed in the B-1 and B-2 steels. The aspect ratio of length to thickness in the A-2 steel is larger than that in the A-1 steel. Takata et al. [16] investigated that the anisotropy was decreased and the mechanical properties was improved as the aspect ratio decreased.

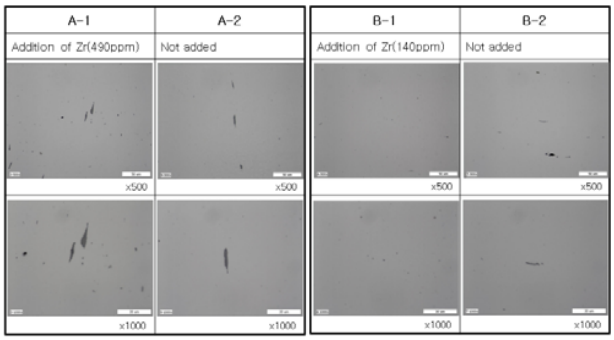

Fig. 5 Optical micrographs of inclusions in the normalized samples

Fig. 6 shows the SEM micrographs of inclusion particles in the normalized A-1 and A-2 samples. A white colored Zr inclusion in MnS particle is observed in the A-1 steel (Fig. 6 (a)) whereas an elongated MnS inclusion is mainly observed in the A-2 steel (Fig. 6(b)). MnS-Zr complex inclusion and rectangular- shaped Zr inclusion were confirmed by SEM-EDS analysis. But no Zr sulfide was observed.

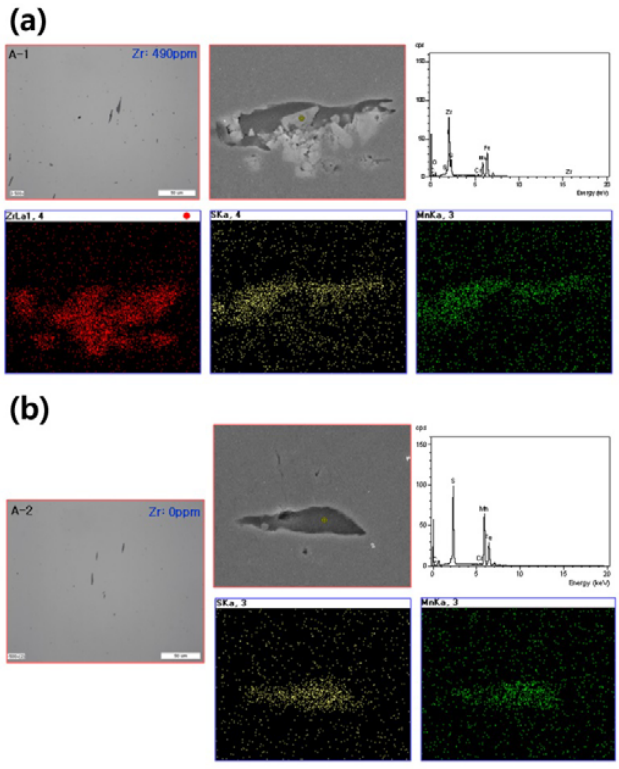

Fig. 6 SEM images and EDS analysis of MnS-Zr inclusions in the normalized (a) A-1 and (b) A-2 steels

IV. Conclusions

(1) The bainitic microstructure was mainly observed in the normalized Cr-Mo plastic mold steels. A large volume fraction of the UB was observed in the low-alloyed A-1 and A-2 steels while a large volume fraction of the LB was observed in the high-alloyed B-1 and B-2 steels. The increased LB fraction caused the higher hardness value.

(2) The strength and hardness of the tempered samples were decreased and the elongation was increased as increasing the tempering temperature. On the other hand, the lowest impact energy was obtained due to the temper embrittlement at 400°C. The alloy additions of Cr, Mo, and V improved the resistance to the temper embrittlement.

(3) The addition of Zr improved the tensile strength and yield strength, but the impact energy was sharply decreased. It may be caused by the formation of Zr-MnS inclusion and rectangular-shaped Zr inclusion due to the Zr addition.

References

[1] K. Narita, Y. Yamaguchi, N. Yagi, and T. Shimohata, "Resulphurized steels containing zirconium," *Tetsu-to-hagané*, vol. 62, pp. 885–894, 1976.

[2] T. Sawai, M. Wakoh, and S. Mizoguchi, "Effect of Zr-oxide particles on the MnS precipitation in low S steels," *Tetsu-to-hagané*, vol. 82, pp. 587–592, 1996.

[3] M. Wakoh, T. Sawai, and S. Mizoguchi, "Effect of Ti-Zr oxide particles on MnS precipitation in low S steels," *Tetsu-to-hagané*, vol. 82, pp. 593–598, 1996.

[4] H. Hasegawa, K. Nakajima, and S. Mizoguchi, "The effects of inclusions in steel on MnS precipitation in Fe-Si alloys," *Tetsu-to-hagané*, vol. 87, pp. 700–706, 2001.

[5] K. Kato, "On the deformation of sulfides in high-sulphur steels by working and the effect of Zr addition," *Tetsu-to-hagané*, vol. 48, pp. 753–761, 1962.

[6] Z. Tang and W. Strumpf, "The role of molybdenum additions and prior deformation on acicular ferrite formation in microalloyedNb-Ti low-carbon line-pipe steels," *Mater. Charac.*, vol. 59, pp. 717–728, 2008.

[7] M. Honjo and Y. Saito, "Numerical simulation of phase separation in Fe-Cr binary and Fe-Cr-Mo ternary alloys with use of the Cahn-Hilliard equation," *ISIJ Inter.*, vol. 40, pp. 914–919, 2000.

[8] B.S. Lement, B.L. Averbach, and M. Cohen, "Microstructural changes on tempering iron-carbon alloys," *Trans. ASM*, vol. 46, pp. 851–881, 1954.

[9] C.J. Altstetter, M. Cohen, and L. Averbach, "Effect of silicon on the tempering of AISI 43XX steels," *Trans. ASM*, vol. 55, pp. 287–300, 1962.

[10] G. Thomas, "Retained austenite and tempered martensiteembrittlement," *Metall. Trans.*, vol. 9, pp. 439–450, 1978.

[11] J.P. Materkowski and G. Krauss, "Tempered martensiteembrittlement in SAE 4340 steel," *Metall. Trans.*, vol. 10, pp. 1643–1651, 1979.

[12] R.M. Horn and R.O. Ritchi, " Mechanisms of tempered martensiteembrittlement in low alloy steels," *Metall. Trans.*, vol. 9, pp. 1039–1053, 1978.

[13] C.L. Braiant and S.K. Banerji, "Phosphorus induced 350°C embrittlement in an ultra-high strength steel," *Metall. Trans.*, vol. 10, pp. 123–126, 1979.

[14] C.L. Braiant and S.K. Banerji, "Tempered martensiteembrittlement in phosphorus doped steels," *Metall. Trans.*, vol. 10, pp.1729–1737, 1979.

[15] C.L. Braiant and S.K. Banerji, "Tempered martensiteembrittlement in a high purity steel," *Metall. Trans.*, vol. 10, pp. 1151–1155, 1979.

[16] H. Takada, K, Kaneco, T. Inoue, and S. Kinoshita, "Effect of shape of MnS inclusion on ductility of rolled plate," *Tetsu-to-hagané*, vol. 62, pp. 866–874, 1976.